

Research Article

Determination of Gypenoside A and Gypenoside XLIX in Rat Plasma by UPLC-MS/MS and Applied to the Pharmacokinetics and Bioavailability

Yan He,¹ Qishun Liang,² Lvqi Luo,² Yifan He,² Xueli Huang,³ and Congcong Wen² 

¹The Molecular Neuropharmacology Laboratory and the Eye-Brain Research Center, The State Key Laboratory of Ophthalmology, Optometry and Vision Science, Wenzhou Medical University, Wenzhou, China

²Laboratory Animal Center, Wenzhou Medical University, Wenzhou, China

³Analytical and Testing Center, School of Pharmaceutical Sciences, Wenzhou Medical University, Wenzhou, China

Correspondence should be addressed to Congcong Wen; bluce494949@wmu.edu.cn

Received 4 April 2022; Revised 21 July 2022; Accepted 23 July 2022; Published 12 August 2022

Academic Editor: Sheng Tang

Copyright © 2022 Yan He et al. This is an open access article distributed under the Creative Commons Attribution License, which permits unrestricted use, distribution, and reproduction in any medium, provided the original work is properly cited.

In this work, a UPLC-MS/MS method was developed for the determination of gypenoside A and gypenoside XLIX in rat plasma. For chromatographic separation, a UPLC BEH C18 column was employed, the mobile phase comprised acetonitrile: water (w/ 0.1% formic acid), and the elution time was 4 min. Detection of each compound was enabled by electrospray ionization in negative-ion mode, and quantitative analysis was enabled by operating in multiple reaction monitoring (MRM) mode by monitoring the transitions of m/z 897.5 \rightarrow 403.3 for gypenoside A, m/z 1045.5 \rightarrow 118.9 for gypenoside XLIX, and m/z 825.4 \rightarrow 617.5 for the internal standard. The calibration curves for gypenoside A and gypenoside XLIX demonstrated excellent linearity ($r > 0.995$) over the range of 2–3000 ng/mL. The intraday and interday precisions of gypenoside A and gypenoside XLIX were within 14.9%, the intraday and interday accuracies ranged from 90.1% to 113.9%, the recoveries were all greater than 88.3%, and the matrix effect ranged from 87.1% to 94.1%. The developed method was successfully applied in the determination of the pharmacokinetics of gypenoside A and gypenoside XLIX. Gypenoside A and gypenoside XLIX had very short half-lives in rats, with oral $t_{1/2z}$ of 1.4 ± 0.2 h and 1.8 ± 0.6 h, respectively, and low bioavailabilities (0.90% and 0.14%, respectively).

1. Introduction

Gynostemma pentaphyllum Makino, also known as five-leaf ginseng and horse chestnut gall [1], is a perennial trailing herb and member of the Cucurbitaceae family of flowering plants [2, 3]. *Gynostemma pentaphyllum* Makino is known to produce a variety of dammarane-type gypenosides [4–6], which have been shown to display antioxidant, antiinflammatory, immunogenic, hypolipidemic, and hypoglycemic effects [7–11]. Gypenosides have also demonstrated protective effects against neurological diseases, such as Alzheimer's disease, Parkinson's disease, depression, and hypoxic brain injury [12–14].

Gypenoside A and gypenoside XLIX are the two main saponins found in *Gynostemma pentaphyllum* [15, 16] and have been isolated from the plant and purified by LC-MS/MS.

Guo et al. performed a solid-phase extraction method and developed an LC-MS/MS method to detect gypenoside XLIX in rat plasma [15]. They then studied the rat pharmacokinetics of gypenoside XLIX after intravenous administration. Hu et al. developed a quantitative UPLC-MS method to detect gypenoside A in rat plasma [17]. Each sample required 5 min, the proteins were precipitated with methanol to avoid interference from matrix effects, and the gypenoside A concentration in rats was determined after oral administration of Gelan-xinning soft capsules. However, both methods only analyzed the *in vivo* concentration of gypenoside A or gypenoside XLIX separately, and neither detected them simultaneously nor did they conduct bioavailability studies.

In this paper, we developed a UPLC-MS/MS method to enable the simultaneous determination of gypenoside A and

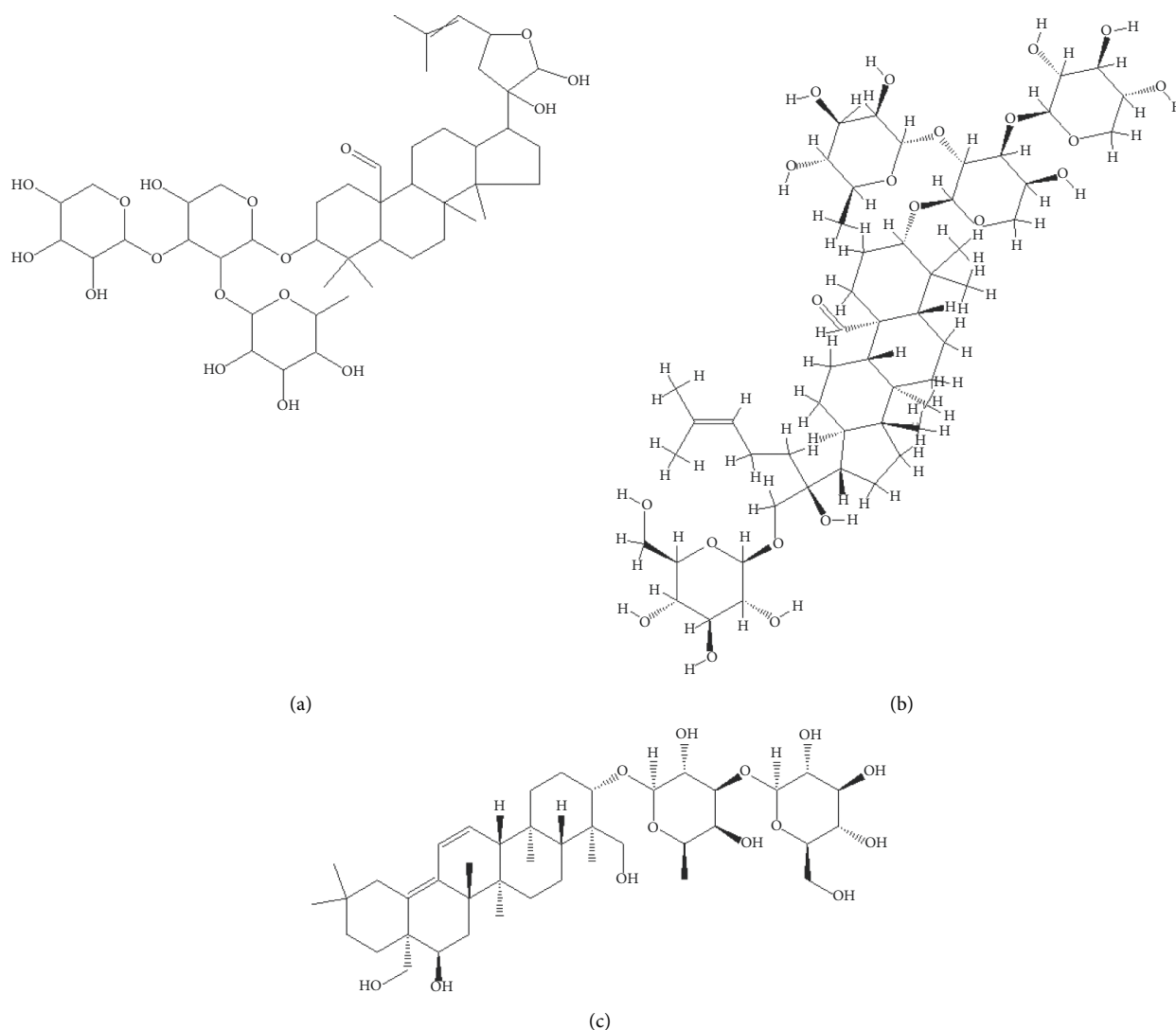


FIGURE 1: Chemical structure of gypenoside A (a), gypenoside XLIX (b), and saikosaponin B2 (c), the internal standard.

gypenoside XLIX in rat plasma and then utilized the method to study the pharmacokinetics of both gypenosides under different administration routes (oral and intravenous administration) to determine their bioavailability.

2. Experimental

2.1. Reagents. Gypenoside A (purity $\geq 98\%$, Figure 1(a)), gypenoside XLIX (purity $\geq 98\%$, Figure 1(b)), and saikosaponin B2 (internal standard, purity $\geq 98\%$, Figure 1(c)) were purchased from Chengdu Mansite Pharmaceutical Co., Ltd. (Chengdu, China). HPLC-grade methanol and acetonitrile were purchased from Merck KGaA (Darmstadt, Germany). Ultrapure water (resistance >18 m Ω) was used to prepare all solutions in this study and was prepared using a Milli-Q purification system (Bedford, MA, USA).

2.2. Instrument Conditions. An ACQUITY I-Class ultra-performance liquid chromatography system coupled with a

Waters XEVO TQ-S microtriple quadrupole tandem mass spectrometer was employed for the detection of gypenosides A and XLIX. The ACQUITY I-Class UPLC system was equipped with a UPLC BEH C18 column (50 mm \times 2.1 mm, 1.7 μ m), and the column temperature was set to 40°C. The mobile phase consisted of a gradient elution of acetonitrile: water (w/0.1% formic acid), the flow rate was 0.4 mL/min, and the elution time was 4 min. Gradient elution profile consisted of 10% acetonitrile, 0–0.2 min; 10–70% acetonitrile, 0.2–1.0 min; 70–90% acetonitrile, 1.0–2.5 min; 90–10% acetonitrile, 2.5–2.8 min; 10% acetonitrile, 2.8–4.0 min.

For the mass spectrometer, nitrogen was used as the cone gas (50 L/h flow rate) and desolvation gas (1000 L/h flow rate). The capillary voltage was set to 3.2 kV, the ion source temperature was 145°C, and the desolvation temperature was 500°C. The mass spectrometer was operated in electrospray (ESI) negative-ion mode, and the quantitation of the two gypenosides was enabled by operating in multiple reaction monitoring modes (MRM) by monitoring the transitions of m/z 897.5 \rightarrow 403.3 (cone voltage 76 V,

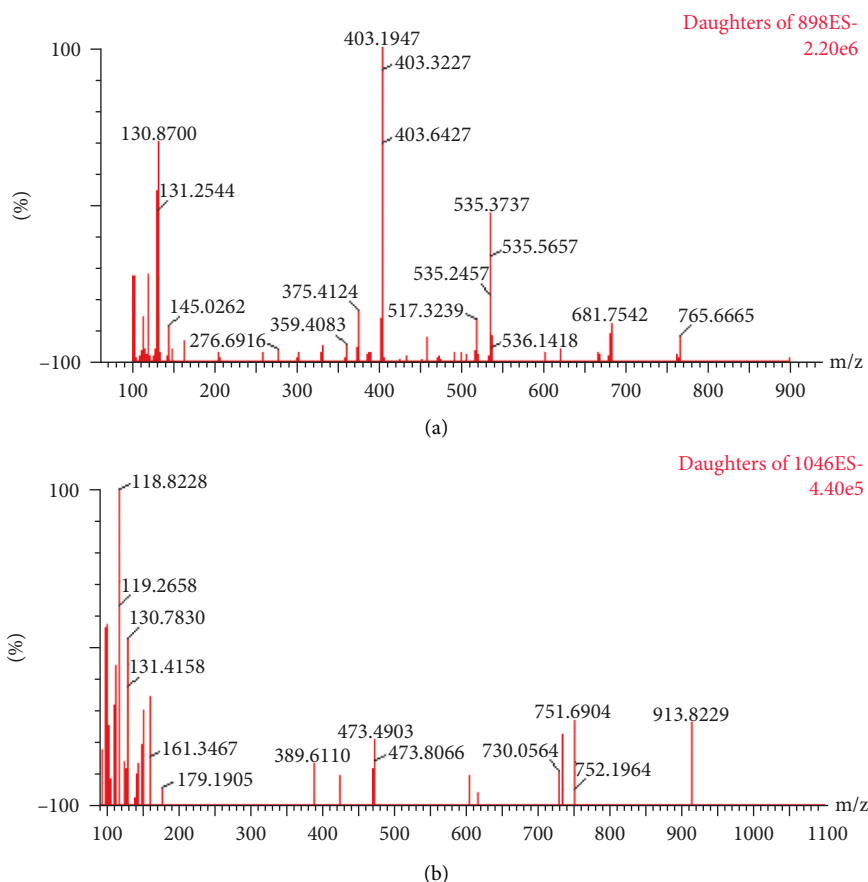


FIGURE 2: Mass spectra of gypenoside A (a) and gypenoside XLIX (b).

collision voltage 40 V) for gypenoside A (Figure 2(a)), m/z 1045.5 \rightarrow 118.9 (cone voltage 70 V, collision voltage 70 V) for gypenoside XLIX (Figure 2(b)), and m/z 825.4 \rightarrow 617.5 (cone voltage 22 V, collision voltage 42 V) for the internal standard.

2.3. Standard Curve. Stock solutions (500 $\mu\text{g/mL}$) of gypenoside A, gypenoside XLIX, and the internal standard were prepared in methanol. The stock solutions were diluted with methanol to obtain working solutions of gypenoside A and gypenoside XLIX at a range of concentrations (20, 100, 200, 500, 2000, 5000, 10000, 20000, and 30000 ng/mL). All stock and working solutions were stored at 4°C. The gypenoside A and gypenoside XLIX working solutions were diluted into blank rat plasma to obtain a series of solutions of the two gypenosides in rat plasma with concentrations of 2, 10, 20, 50, 200, 500, 1000, 2000, and 3000 ng/mL . Quality control (QC) samples were also prepared in blank rat plasma at different concentrations (5, 250, and 2500 ng/mL) under the same conditions.

2.4. Sample Preparation. To prepare the plasma samples, 50 μL of rat plasma was added to a 1.5 mL Eppendorf tube, to which 150 μL of acetonitrile-methanol (9:1, v/v) (containing 100 ng/mL of the internal standard) was added. The

solutions were vortexed for 1.0 min and centrifuged at 13000 rpm for 10 min at 4°C. An aliquot (100 μL) of the supernatant was transferred to a lined tube of the injection bottle, and 3 μL of the solution was injected into the UPLC for UPLC-MS/MS analysis.

2.5. Pharmacokinetics. Sprague Dawley (SD) rats (male, 220–250 g) were obtained from the Animal Experiment Center of Wenzhou Medical University (Wenzhou, China). All experimental procedures and protocols were approved by the Animal Care Committee of Wenzhou Medical University. Six rats were administered gypenoside A was administered intravenously (iv, 1 mg/kg) and orally (po, 5 mg/kg), and another six rats were administered the same dosages of gypenoside XLIX, for a total of 12 rats. At 0.0833, 0.25, 1, 2, 4, 6 h (for gypenoside A) and 0.0833, 0.25, 1, 2, 4, 6, 8, 12 h (for gypenoside XLIX) postadministration, 0.2 mL of blood was collected from the caudal (tail) vein into heparinized Eppendorf tubes, which were centrifuged at 13000 rpm for 10 min. Then, 50 μL of the plasma (top-most layer) was transferred to a 1.5 mL Eppendorf tube and stored at -80°C until analysis of the pharmacokinetic parameters, which were statistically calculated using the pharmacokinetic DAS 2.0 software. The formula for absolute bioavailability was $\text{AUC for oral administration}/\text{AUC for intravenous administration} \times 100\%$.

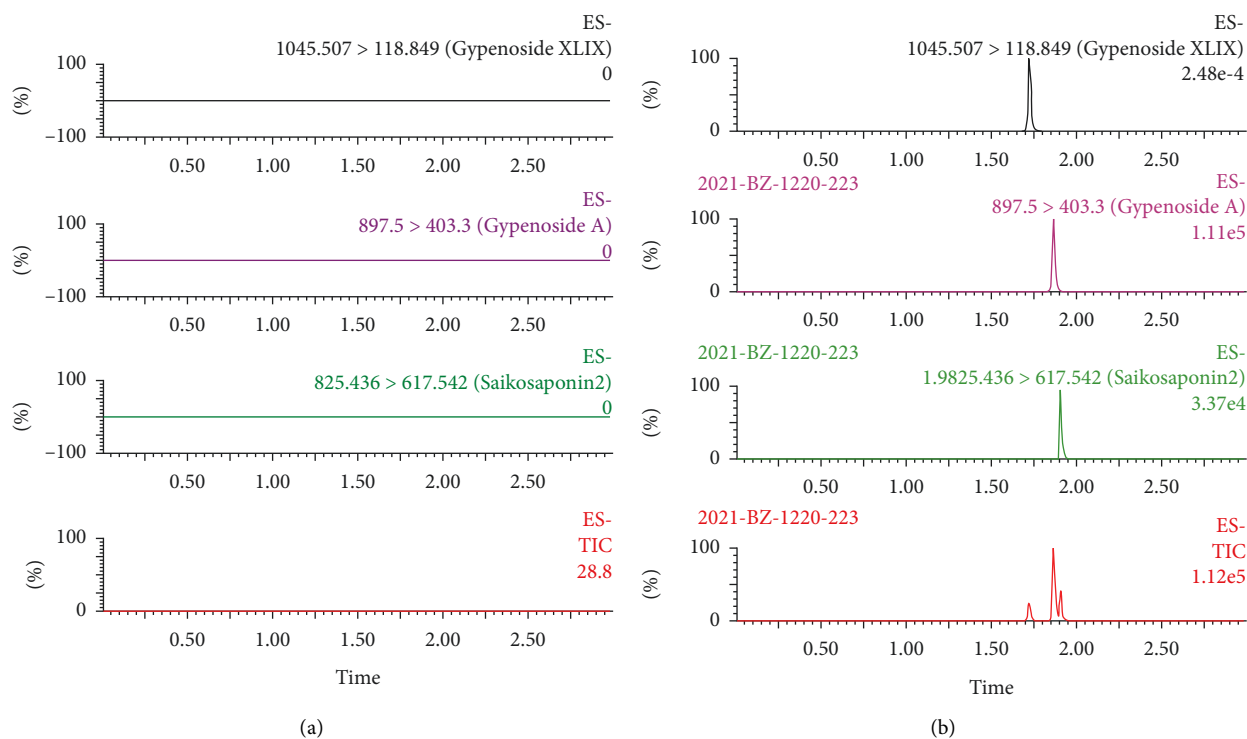


FIGURE 3: UPLC-MS/MS chromatograms of gypenoside A, gypenoside XLIX, and the internal standard in rat plasma (a) and blank rat plasma spiked with gypenoside A, gypenoside XLIX, and internal standard (b).

3. Results and Discussion

3.1. Method Development. The mass spectrometry conditions were obtained after optimizing the spray needle voltage, drying gas temperature, capillary voltage, and collision energy [18–21]. Comparing the positive and negative modes, gypenoside A and gypenoside XLIX were best suited for detection in ESI negative-ion mode because the sensitivity was significantly higher than detection in other modes. Gypenoside A and gypenoside XLIX were prepared in rat blank plasma at a concentration of 100 ng/mL. During the method development, a variety of different solvents and solvent mixtures were assessed for their ability to efficiently precipitate the proteins in the rat plasma. Acetonitrile, methanol-acetonitrile (1:9, v/v), 10% trichloroacetic acid, methanol-acetonitrile (1:1, v/v), and methanol were employed, and it was determined that methanol-acetonitrile (1:9, v/v) had the highest extraction efficiency, so it was chosen as the solvent for the protein precipitation step.

3.2. Selectivity. As shown in Figure 3, the retention times of gypenoside A, gypenoside XLIX, and the internal standard were 1.86, 1.72, and 1.91 min, respectively, and there was no interference from the endogenous components within the plasma, indicating that the developed method was highly selective for the two natural compounds.

3.3. Standard Curve. The calibration curves of gypenoside A and gypenoside XLIX in rat plasma that were generated over the concentration range of 2–3000 ng/mL demonstrated

excellent linearity, indicating that they could reliably be used for calculating the concentration of the natural compounds in the rat plasma. The regression equation for gypenoside A was $y_1 = 0.0096x_1 + 0.0023$ ($R^2 = 0.9984$), wherein x_1 represented the concentration of gypenoside A in the plasma, and y_1 represented the ratio of the peak area of gypenoside A to the internal standard. The regression equation for gypenoside XLIX was $y_2 = 0.0024x_2 + 0.0014$ ($R^2 = 0.9971$), wherein x_2 represented the concentration of gypenoside XLIX in plasma, and y_2 represented the ratio of the peak area of gypenoside XLIX to the internal standard. Based on these two equations, the lower limit of quantification of gypenoside A and gypenoside XLIX in rat plasma was 2 ng/mL, and the detection limit was 1 ng/mL.

3.4. Precision, Accuracy, Recovery, and Matrix Effects. The intraday and interday precisions of gypenoside A were within 14.9%, the intraday and interday accuracies were 90.1–107.5%, the recovery was greater than 88.3%, and the matrix effects were 87.1–93.9%. The intra- and interday precisions of gypenoside XLIX were within 12.9%, the intra- and interday accuracies were 91.8–113.9%, the recovery was greater than 93.2%, and the matrix effects were in the range of 89.3–94.1% (Table 1).

3.5. Stability. The accuracy of gypenoside A was between 92.2% and 110.3%, and the RSD was within 14.8%; the accuracy of gypenoside XLIX was between 87.9% and 112.2%, and the RSD was within 14.5% (Table 2). These

TABLE 1: Accuracy, precision, matrix effect, and recovery of gypenoside A and gypenoside XLIX in rat plasma.

Compound	Concentration (ng/mL)	Accuracy (%)		Precision (RSD%)		Matrix effect (%)	Recovery (%)
		Intraday	Interday	Intraday	Interday		
Gypenoside A	2	90.1	107.5	13.8	14.9	89.9	92.7
	5	103.2	90.5	7.0	6.4	93.5	88.3
	250	100.0	102.9	8.5	7.9	93.9	95.0
	2500	101.8	103.3	6.1	9.9	87.1	89.4
	2	91.8	113.9	10.4	12.9	90.4	97.1
Gypenoside XLIX	5	108.9	94.2	8.1	10.4	92.9	94.4
	250	106.2	106.1	8.1	11.3	94.1	93.2
	2500	99.3	94.2	6.1	4.4	89.3	98.2

TABLE 2: Stability of gypenoside A and gypenoside XLIX in rat plasma (%).

Compound	Concentration (ng/mL)	Autosampler (4°C, 12 h)		Ambient (2 h)		-20°C (30 d)		Freeze-thaw	
		Accuracy	RSD	Accuracy	RSD	Accuracy	RSD	Accuracy	RSD
Gypenoside A	5	101.9	7.8	93.7	9.2	102.7	13.3	110.3	14.8
	250	100.5	2.8	99.9	5.3	93.8	7.2	108.6	7.2
	2500	96.6	5.6	106.0	5.6	99.8	5.9	92.2	6.0
	5	101.1	11.7	107.7	11.5	112.2	14.5	91.2	13.3
Gypenoside XLIX	250	108.6	8.4	97.4	6.5	90.7	7.9	87.9	13.0
	2500	99.5	8.0	95.5	8.8	88.0	1.4	103.9	9.5

TABLE 3: Main pharmacokinetic parameters after intravenous (iv) and oral (po) administration of gypenoside A and gypenoside XLIX in rats.

Compound	Group	AUC _(0-t) (ng/mL·h)	AUC _(0-∞) (ng/mL·h)	t _{1/2z} (h)	CL _{z/F} (L/h/kg)	V _{z/F} (L/kg)	C _{max} (ng/mL)
Gypenoside A	Po, 5 mg/kg	14.9 ± 2.4	15.9 ± 2.5	1.4 ± 0.2	319.9 ± 49.8	665.4 ± 161.4	8.6 ± 1.3
	Iv, 1 mg/kg	332.9 ± 31.2	334.3 ± 32.2	0.8 ± 0.2	3.0 ± 0.3	3.3 ± 0.7	621.9 ± 36.2
Gypenoside XLIX	Po, 5 mg/kg	13.7 ± 2.5	15.4 ± 2.2	1.8 ± 0.6	330.8 ± 52.7	879.8 ± 345.0	8.1 ± 0.9
	Iv, 1 mg/kg	1923.5 ± 62.5	1926.6 ± 62.3	1.6 ± 1.7	0.52 ± 0.02	1.2 ± 1.3	2201.9 ± 211.6

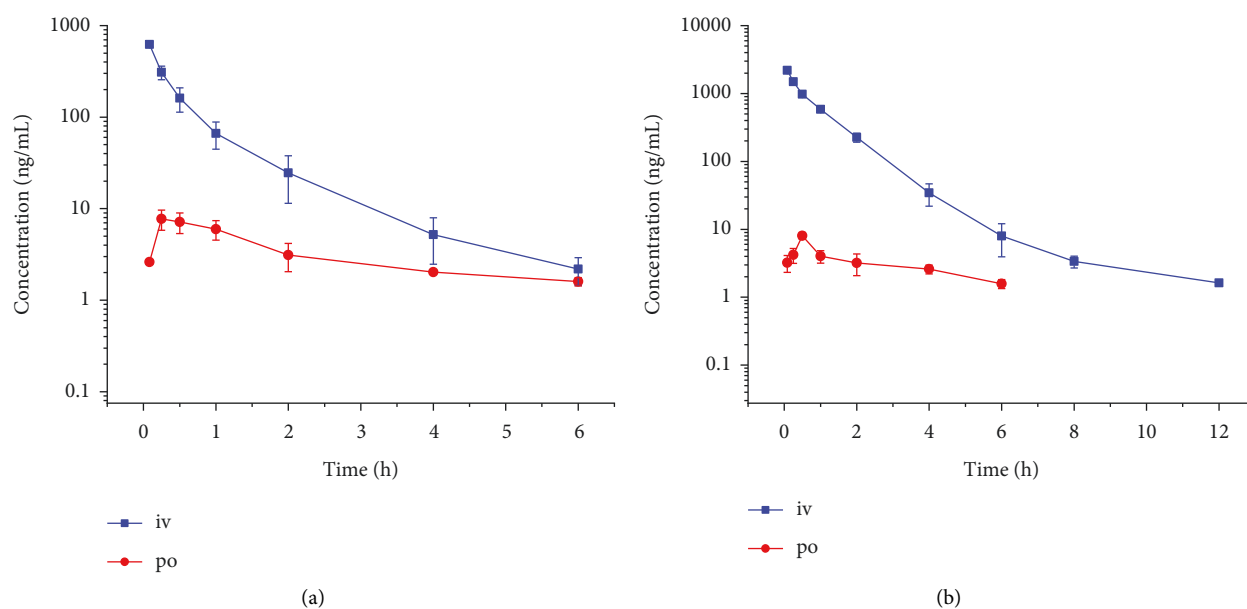


FIGURE 4: The concentration-time curve of rats after intravenous (iv, 1 mg/kg) and oral (po, 5 mg/kg) administration of gypenoside A (a) and gypenoside XLIX (b).

results indicated that gypenoside A and gypenoside XLIX had excellent stability.

3.6. Pharmacokinetic Studies. The noncompartmental model was used to fit the main pharmacokinetic parameters (Table 3), and the concentration-time curves for gypenoside A and gypenoside XLIX in rat plasma are shown in Figure 4. After intravenous administration, the half-lives ($t_{1/2z}$) of gypenoside A and gypenoside XLIX in the rats were 0.8 ± 0.2 h and 1.6 ± 1.7 h, respectively, while the oral $t_{1/2z}$ were 1.4 ± 0.2 h and 1.8 ± 0.6 h, respectively, indicating that the compounds were metabolized very quickly. The $t_{1/2}$ of gypenoside A in rats reported in the literature was 6.247 ± 2.039 h [17], which is significantly longer than the values we reported, but this difference was likely due to the different dosage forms. However, the $t_{1/2}$ of gypenoside XLIX in rats reported in the literature (3.17 ± 1.01 h) was closer to the values we calculated [15]. Based on the pharmacokinetics data, gypenoside A and gypenoside XLIX had very low oral bioavailabilities of 0.90% and 0.14%, respectively, indicating that the concentration of the drug in systemic circulation was low.

4. Conclusion

In this study, a UPLC-MS/MS method was established for the determination of gypenoside A and gypenoside XLIX in rat plasma. The UPLC-MS/MS method required only 4 min for each sample, and a simple and inexpensive protein precipitation method was used. The accuracy, precision, selectivity, and linearity of this method were highly robust, corroborating the application of this method in studying the pharmacokinetics and bioavailability of these compounds and others alike in rats.

Data Availability

The data used to support the findings of this study are included within the article.

Conflicts of Interest

The authors declare that there are no conflicts of interest regarding the publication of this paper.

Acknowledgments

This work was supported by the Young Talent Project of Wenzhou Medical University.

References

- [1] Y. Zhang, Q. Chen, Y. Huang et al., "Gene excavation and expression analysis of CYP and UGT related to the post modifying stage of gypenoside biosynthesis in *Gynostemma pentaphyllum* (Thunb.) Makino by comprehensive analysis of RNA and proteome sequencing," *PLoS One*, vol. 16, no. 12, Article ID e0260027, 2021.
- [2] K. Li, C. Ma, H. Li, S. Dev, J. He, and X. Qu, "Medicinal value and potential therapeutic mechanisms of *Gynostemma pentaphyllum* (thunb.) Makino and its derivatives: an overview," *Current Topics in Medicinal Chemistry*, vol. 19, pp. 2855–2867, 2019.
- [3] L. Wang, M. Pang, X. Wang, P. Wang, Y. Xiao, and Q. Liu, "Characteristics, composition, and antioxidant activities in vitro and in vivo of *Gynostemma pentaphyllum* (Thunb.) Makino seed oil," *Journal of the Science of Food and Agriculture*, vol. 97, no. 7, pp. 2084–2093, 2017.
- [4] T. X. Wang, M. M. Shi, and J. G. Jiang, "Bioassay-guided isolation and identification of anticancer and antioxidant compounds from *Gynostemma pentaphyllum* (Thunb.) Makino," *RSC Advances*, vol. 8, no. 41, pp. 23181–23190, 2018.
- [5] X. Wang, D. Li, X. Guo et al., "ComMS(n)DB-An automatable strategy to identify compounds from MS data sets (identification of gypenosides as an example)," *Journal of Agricultural and Food Chemistry*, vol. 68, no. 41, pp. 11368–11388, 2020.
- [6] X. Weng, Y. Y. Lou, Y. S. Wang et al., "New dammarane-type glycosides from *Gynostemma pentaphyllum* and their lipid-lowering activity," *Bioorganic Chemistry*, vol. 111, Article ID 104843, 2021.
- [7] X. Shang, Y. Chao, Y. Zhang, C. Lu, C. Xu, and W. Niu, "Immunomodulatory and antioxidant effects of polysaccharides from *Gynostemma pentaphyllum* Makino in immunosuppressed mice," *Molecules*, vol. 21, no. 8, p. 1085, 2016.
- [8] H. P. Wu and Y. K. Lin, "Effect of *Eucommia ulmoides* Oliv., *Gynostemma pentaphyllum* (Thunb.) Makino, and *Curcuma longa* L. on Th1- and Th2-cytokine responses and human leukocyte antigen-DR expression in peripheral blood mononuclear cells of septic patients," *Journal of Ethnopharmacology*, vol. 217, pp. 195–204, 2018.
- [9] B. Wang, J. Niu, B. Mai et al., "Effects of extraction methods on antioxidant and immunomodulatory activities of polysaccharides from superfine powder *Gynostemma pentaphyllum* Makino," *Glycoconjugate Journal*, vol. 37, no. 6, pp. 777–789, 2020.
- [10] Y. Li, J. Huang, W. Lin et al., "In Vitro Anticancer activity of a nonpolar fraction from *Gynostemma pentaphyllum* (thunb.) Makino," *Evidence-based Complementary and Alternative Medicine*, vol. 2016, pp. 1–11, 2016.
- [11] Y. Li, W. Lin, J. Huang, Y. Xie, and W. Ma, "Anti-cancer effects of *Gynostemma pentaphyllum* (thunb.) Makino (jiaogulan)," *Chinese Medicine*, vol. 11, no. 1, p. 43, 2016.
- [12] T. T. Zhao, K. S. Kim, K. S. Shin et al., "Gypenosides ameliorate memory deficits in MPTP-lesioned mouse model of Parkinson's disease treated with L-DOPA," *BMC Complementary and Alternative Medicine*, vol. 17, no. 1, 2017.
- [13] K. S. Shin, T. T. Zhao, K. H. Park et al., "Gypenosides attenuate the development of L-DOPA-induced dyskinesia in 6-hydroxydopamine-lesioned rat model of Parkinson's disease," *BMC Neuroscience*, vol. 16, no. 1, p. 23, 2015.
- [14] K. S. Shin, T. T. Zhao, H. S. Choi, B. Y. Hwang, C. K. Lee, and M. K. Lee, "Effects of gypenosides on anxiety disorders in MPTP-lesioned mouse model of Parkinson's disease," *Brain Research*, vol. 1567, pp. 57–65, 2014.
- [15] S. Guo, C. Sui, and Y. Ma, "Development of a targeted method for quantification of gypenoside XLIX in rat plasma, using SPE and LC-MS/MS," *Biomedical Chromatography*, vol. 31, no. 6, Article ID e3898, 2017.
- [16] T. H. W. Huang, V. H. Tran, B. D. Roufogalis, and Y. Li, "Gypenoside XLIX, a naturally occurring PPAR- α activator, inhibits cytokine-induced vascular cell adhesion molecule-1 expression and activity in human endothelial cells," *European Journal of Pharmacology*, vol. 565, no. 1–3, pp. 158–165, 2007.

- [17] X. Hu, S. Wenjun, G. Xin, and W. Xijing, "Pharmacokinetics of gypenoside A in glanxinning soft capsules in Rats," *Modern Chinese Medicine*, vol. 22, p. 6, 2020.
- [18] W. Sun, X. Jiang, X. Wang, and X. Bao, "Pharmacokinetic study of zhebeirine in mouse blood by ultra- performance liquid chromatography/tandem mass spectrometry," *Current Pharmaceutical Analysis*, vol. 17, no. 4, pp. 547–553, 2021.
- [19] Q. Zhou, Z. G. Zhang, P. Geng, B. G. Huang, X. Q. Wang, and X. M. Yu, "Pharmacokinetics of ligustroflavone in rats and tissue distribution in mice by UPLC-MS/MS," *Acta Chromatographica*, vol. 32, no. 2, pp. 102–106, 2020.
- [20] H. C. Zhan, Z. Wei, K. Ren, S. H. Tong, X. Q. Wang, and Q. Wu, "Pharmacokinetics of isocorynoxine in rat plasma after intraperitoneal administration by UPLC-MS/MS," *Acta Chromatographica*, vol. 32, no. 4, pp. 260–263, 2020.
- [21] B. X. Weng, Z. Q. Zhong, Y. Yu, J. Lin, and C. C. Wen, "Determination and pharmacokinetics of cepharanthine in rat plasma by UPLC-MS/MS," *Latin American Journal of Pharmacy*, vol. 39, pp. 1100–1104, 2020.